PAPER Nr.: 71

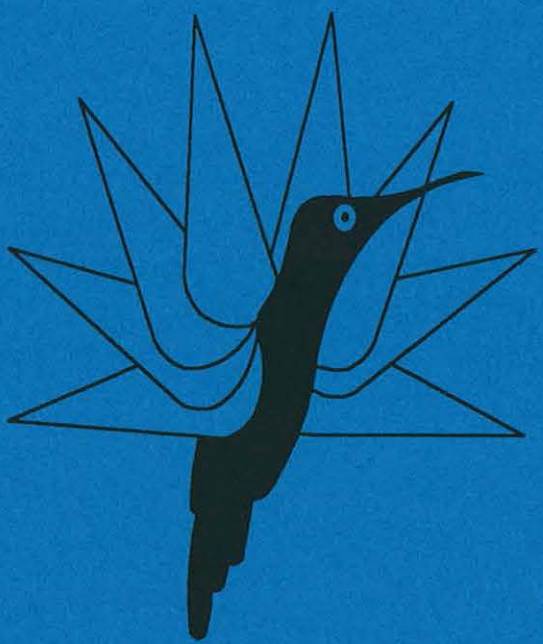

THEORETICAL INVESTIGATIONS AND WINDTUNNEL TESTS WITH HHC-IBC

BY

P. RICHTER AND T. SCHREIBER

ZF LUFTFAHRTTECHNIK GMBH
KASSEL/CALDEN, GERMANY

TWENTIETH EUROPEAN ROTORCRAFT FORUM
OCTOBER 4 - 7, 1994 AMSTERDAM

Printed by the Technical Highschool Haarlem

THEORETICAL INVESTIGATIONS AND WINDTUNNEL TESTS WITH HHC-IBC

P. Richter and T. Schreiber
(ZF Luftfahrttechnik GmbH, Kassel, Germany)

Abstract

The development of an Individual Blade Control device for advanced main rotor controls has reached its culmination with the open loop tests of the Bo105 fullscale behaviour in the 80x40ft-windtunnel at NASA Ames in 1993/94.
Due to these times higher control authorities the effects could be pointed out much clearer as seen in the former flight tests (MBB, HFW). By the hand they are a welcome complement to the constructive efforts towards an optimized closed-loop-control for monofrequent and mixed-mode operations.
The presentation of the corrected measurements in comparance with simulated results apply a better knowledge of the capacity on vibration, noise, and shaft power reduction under regardance of blade and hub load limits as well as the influence of stall flutter and other dynamic and aerodynamical effects.
It is shown that the rotor conditions have got an elementary influence on effects aimed by modified blade controls. A fact that was introduced in the continuing tests in spring 1994 and regarded in this paper.
Future goals will lead to a coupling of several tasks especially vibration reduction and enlargement of flight envelopment as well as noise reduction coupled with retrim options.

Notations and Abbreviations

C_L , C_D , C_M	lift, drag and moment coefficient
$C_{L\alpha}$	lift curve slope
C_T	thrust coefficient
d_{SD}	structural damping factor
$\underline{F}$	load vector
$\underline{i}$, $\underline{j}$, $\underline{k}$	blade element inertial system
L , M	aerodynamic lift and moment
$\underline{M}$	load matrix
r , x	local radius coordinate, x=r/R
R	rotor radius
s	integration coordinate
u , v , w	inflow components
U	rotor tip speed, ΩR
v_n , v_t , v_r	normal, tangential and radial blade inflow
V	velocity
w_i	induced velocity
$\underline{w}$	cantilever blade bending
x , z , r	blade coordinates
X, Y, Z, M, N	hub loads
α	angle of attack
β , ζ, θ	flap, lead-lag and torsion angle
ε	tolerance
Γ	circulation
ϑ	blade pitch angle
$\underline{\Theta}_{IBC}$	IBC control vector
φ	feedback phase
μ	advance ratio, v/U
ρ	specific blade mass
σ	solidity
τ	time constant for stall delay
ψ	blade azimut angle
Ω	rotor rotational speed

aero	aerodynamic
basel	baseline
cos4Ω	cos-component of vibration
bl	blade
d	delayed
inst	instationary
mass	inertial
meas	measurement
mod	modified
res	resultant
sin4Ω	sin-component of vibration
targ	target
vib	vibrational
nΩ	coupled to n^{th} control input
$\dot{(\,)}$	$\delta(\,)/\delta t$
$(\,)'$	$\delta(\,)/\delta x$

1. Introduction

Today's helicopters have taken their part in modern aviation for special tasks of vertical take off, landing and hovering. In spite of the advanced technologies developed in recent years some of the major problems like vibrations, high power consumption, and increased noise emissions still remain due to the complex mechanical interaction and nonuniform aerodynamic downwash. These effects lead to a lack of acceptance for helicopters in economy and public.

However a large spectrum of missions coupled with the permanent change of rotor interferences discriminates structural and passive means for the reduction of those effects because they normally only act on certain flight conditions. Therefore this cannot be a solution for the entire problem.
A more competitive possibility seems to be offered by the development of active control systems. To reduce the phenomena at the origin an accomplishment to the existing collective and cyclic control, realized by the mechanical behavior of the conventional swashplate, had to be introduced.
First steps to the Higher Harmonic Control (HHC) were made in 1964. The conventional control system of an UH-1A was modified beneath the swashplate in a way that multiple frequencies of the rotational speed Ω could be mixed into the normal controls. Unfortunately this system could only act with the $(n-1)^{th}$, n^{th} and $(n+1)^{th}$ higher harmonics of the blade multiharmonics according to the mechanical couplings of the swashplate. The following test shows that the analytically expected reduction of the power gain did not appear due to mispredicted mechanic and aerodynamic response [1]. Only significant effects on the vibrational behaviour could be realized and may have led to stronger efforts of the 70s and 80s in that task.
According to the public interest also the question of noise reduction engaged by the blade vortex interactions (BVI) was treated more seriously, because it can also be influenced by modified blade controls. As can be seen in fig.1 the problems of helicopters are generated by a combination of aerodynamic and rotor dynamic phenomena.

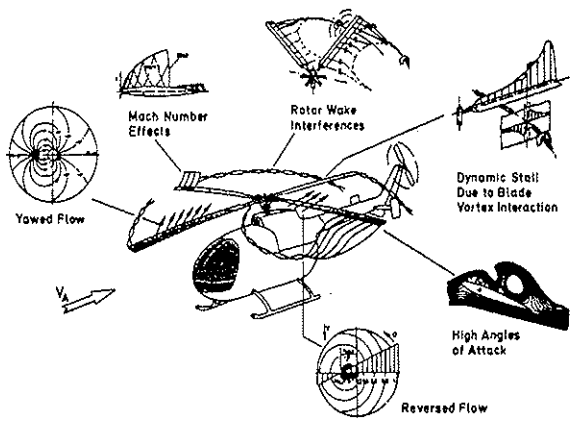

Fig. 1 : Limiting Phenomena of Helicopter Rotors

The main influences on the downwash of a trimmed helicopter are the Mach number effect and the reverse flow of the advancing and retreating blade and in this way with a special excitation every two times of a rotor rotation leading to remarkable influences of the 2Ω-controls. Another phenomenum is the interference of blades and vortices with dynamic and instationary effects. These interferences are also enlarged by blades excited with high frequencies as expected with active blade control systems like HHC.
However, in recent years the helicopter market concentrated more and more on vehicles with more than 3 blades. To avoid the limitation of the dedicated Higher Harmonic Control System a facility of more potential had to be developed.
To get an unlimited individual blade excitation each of it had to be equiped with a single actuator, hydraulic supply and control features.
Since 1984 ZF Luftfahrttechnik GmbH (ZFL, former Henschel Flugzeugwerke) is developing a direct control device on the base of an automatically adjustable control rod [2].

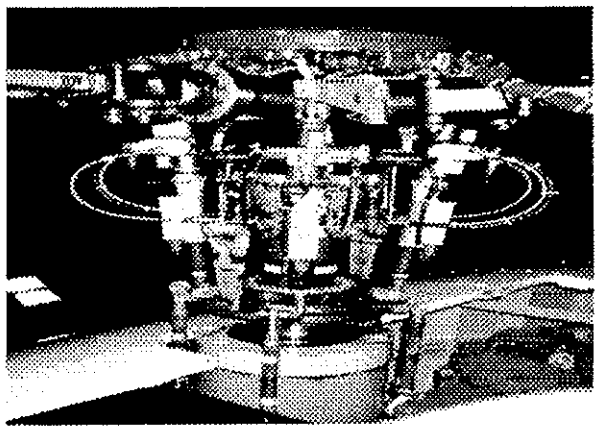

Fig. 2 : Photo of the IBC-System (ZFL) at the RTA

The device in fig. 2 represents the third stage of IBC-development. In addition former versions have already been tested on a whirl tower and on flight tests in cooperation with EUROCOPTER DEUTSCHLAND (ECD) but only with low control authorities ($<1.2°$).
The culmination of the developing efforts was reached at the fullscale windtunnel tests in 1993/94 involved in the German-American Memorandum of Understanding (MOU).
The discussion of the measured data in comparance with theoretical investigations regarding vibrations, performance and noise improvements at the helicopter rotor is the main interest of this presentation.
Finally an estimation of the IBC-systems future potential is given according to the uncompleted data consideration till today.

2. Windtunnel Configuration

In order to test the dedicated improvements with Higher Harmonic Blade Control a fullscale helicopter windtunnel model of the rotortype BO 105 was equiped with an appropriate construction in spring of

1993 and 1994 in the 40x80ft-windtunnel at NASA Ames. The testing-matrix did not only include the high flying speed and thrust loads, but also was expanded to the whole flight area of the Bo105 helicopter which is limited by the rotor performance and thrust efficiency.

The flight performance of a helicopter is mainly influenced by its rotor efficiency under the regardance of stability characteristics and material loads. Above all, the main concern is to achieve a higher air speed and carrying capacity or at least a smaller need of fuel and an extension of range, respectively, keeping the same flight conditions. The vibration- and control loads should not be increased significantly or as far as possible be suppressed. Also blade vortex interactional noise can be influenced.

The measurements of the windtunnel equipment consisted of static data and dynamic derivatives from FFT-analysis of the rotor balance time history. Both were independent of each other. The loads were available for the balance center coordinates but also were computed for other locations like the hub center and the rotating frame.

The blades were equiped with a number of strain gauge devices, accelerometers, and pressure indicators. These devices supplies with a complete blade load, motion and pressure distribution on the rotor disk. The tip displacement and twist was calculated online.

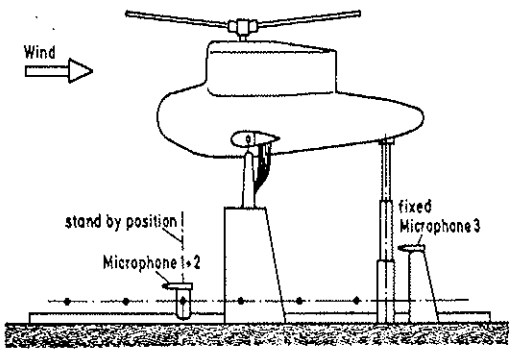

Fig. 3 : NASA-RTA with Microphones and Traverse Position

On the ground of the test rig several microphones were installed together with a movable traverse to get large sound distribution matrices on the advancing blade side.

The IBC-system developed, build, maintained, and controlled by ZF Luftfahrttechnik GmbH, Kassel, was independently operated by the owner but of course in tight coordination with NASA control, who did the conventional trimming as well as fundamental wind tunnel and safety handlings [3].

The inputs of the HHC-IBC were managed by a specially developed digital control unit (ZFL) and supplied signals up to 8Ω, confirmatively. The authority was limited by the hydraulic system but so far beyond the constructive end position. The controls, that were needed for the dedicated tests, didn't ever touch the power limit.In this way there was enough potential for mixed mode operations, where control amplitudes could add up to 3.5° for the maximum.

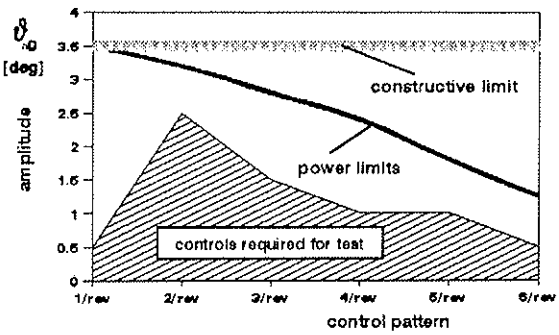

Fig. 4 : Limitations of the IBC-System

The data of the RTA were received by NASA's Rotor Data Reduction System (RDRS). The static data could be used online during the test. The dynamic data normally needed 1 or 2 days to be reduced and corrected.

The NASA also tried to introduce an adaptive control system. But due to the lack of preparance time these results were not very effective. During the test it offered no real improvement and is likely to be a help in future test series.

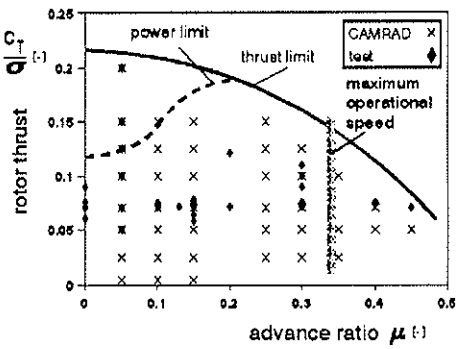

Fig. 5 : Envelope of the Windtunnel tests 1993/94 and the Theoretical Investigations

Several tests were carried out with a constant higher harmonic amplitude and varried input phase angle for single- and multiharmonic controls in the velocity range up to 190kt (μ=0.45) and with a thrust load up

to 40000N (C_T/σ=0.12). Roll- and pitch moments were trimmed flight relevant according to the correlation study of the MOU [4]. The angle of attack of the rotor was chosen in accordance with the flight conditions that needed to be examined. Based on that the effective angle of attack was varried.

2.1 Hardware Problems

During the tests only a few problems with the hardware occured. Normally it was not bound on the IBC-system itself, but more on the supply devices.
There have been two leakages due to adaptation problems that could be managed with simple modifications at the seal.
Another problem arose with the torsional flutter of the IBC-actuators initated by the changes of the aerodynamic load on the advancing and retreating side. It could quickly be solved by a damping tie between the actuator supply connectors. Future configurations are supposed to be protected by the airframe so that this part does not need any further improvements.
A further appearance was the rocking phenomenon at a test velocity of V_{kts}=170kts which declined above and beyond, but had serious effects on trim precision and the load measurements.
To point out the influence some long term measurements of the hub loads were performed. As can be seen in fig. 6 the spectra offer two low frequency peaks that come very close to the mentioned velocity. The reason is obviously an eigen mode of the wind tunnel and the rotor blade motion which come to an interaction at certain circumstances. This generated a rocking effect of the rotor inflow and in this way on the load condition of the entire test stand.

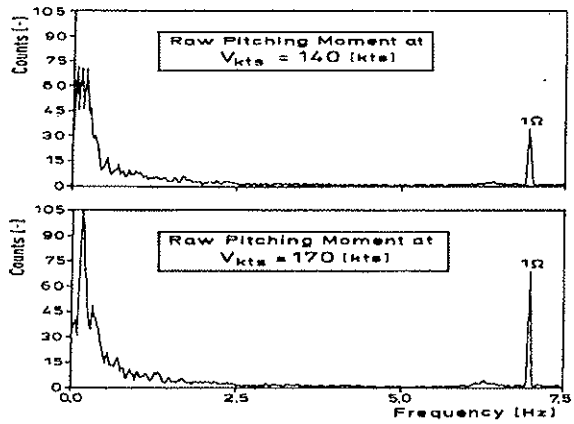

Fig. 6 : Long Term Measurements of the Hub Pitch Moment at Different Tunnel Speed

Unfortunately there was not enough time to point out these effects more clearly. To get more precise results a sequential aquisition of three data points was performed. But the need for that only occured at one velocity condition as proved by latter regardance of the dynamic data.
The inherent security of the actuators was proved by a number of break down tests at the end of the series. Altogether the tests of 1993 and 1994 offered a full range identification with a number of different periodic especially higher harmonic controls of Bo105-rotor in a wind tunnel. The system showed its technical ability for the use in helicopter rotors

3. Simulation of the Wind Tunnel Model

The basis of the simulation results is the analytical Programcode CAMRAD/JA [5]. Detailed investigations of a fully coupled elastic blade with variable geometry, a twodimensional aerodynamic polar curve for a blade element theory and corrections for the registration of 3D-effects as well as the dynamic stall and unsteady aerodynamic loads dependent on the rotor-rotation are included. The parallel solutions will be iteratively led to convergence.
The rotor hub and pitch link can be shaped elasticated and geometrical variable. They allow a consideration of all existing loads and vibrations. The solution is integrated and *FOURIER*-transformed on the basis of an quasi stationary single blade model. The downwash of the rotor is simulated by a potential theoretical free wake model. All considerations are valid only for non accelerated states of the vehicle.

3.1. The Elastic Rotor Blade

In contrast to the hinged substitutional models of other systems [6] the rotor blade of this study is presented by an inhomogeneous engineering beam theory with variable specific root geometry and with full couplement of flap-lag-bending and torsion.

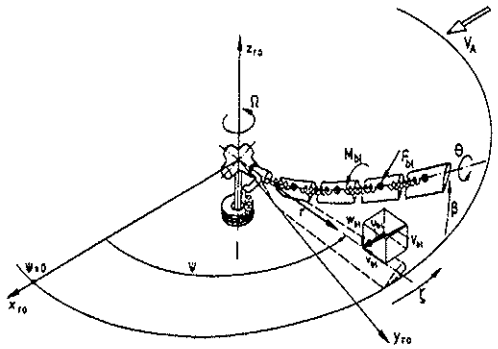

Fig. 7 : Simplified Engineering Beam Model of the Rotor Blade

The elasticity of the mast and control system is con-

sidered by simple spring stiffnesses.
Basis of the inertial and aerodynamic loads as well as the blade motion is a balance of moments in every single of the chosen blade elements refered to the next element with a sectional blade equation.

$$\underline{\underline{M}}_{aero} - \underline{\underline{M}}_{mass} - \underline{\underline{M}}_{elast} = 0 \qquad (1)$$

Elastic loads are named from blade element theory together with structural damping, coupled forces

$$\underline{\underline{M}}_{elast} = [\ E\ I\ ]\ \underline{w}'' + diag[d_{SD}]\ \dot{\underline{w}} \qquad (2)$$

due to gravity

$$\underline{\underline{M}}_{mass} = R \int_{x}^{1} \int_{\Delta x} (\underline{f}(\Omega) - \underline{f}(x)) \times \underline{\ddot{w}}\ dm\ d\Omega \qquad (3)$$

and aerodynamic forces.

$$\begin{aligned} \underline{\underline{M}}_{aero} &= R \int \underline{F}_{aero}\, dx \\ &= R \int \underline{F}_x\, \underline{i}_{Bl} + \underline{F}_z\, \underline{k}_{Bl} + \underline{F}_y\, \underline{j}_{Bl}\, dx \end{aligned} \qquad (4)$$

The blade is calculated with engineering beam theory with discreted blade elements as well as considering a variable geometry and mass distribution up to the response of pitch link geometry [8] nonlinear terms are inserted and are solved by harmonic statements and seperation of variables.

$$\underline{w} = \sum_{n=1}^{\infty} \underline{\underline{A}}_n (x)\ \underline{B}_n (t) \qquad (5)$$

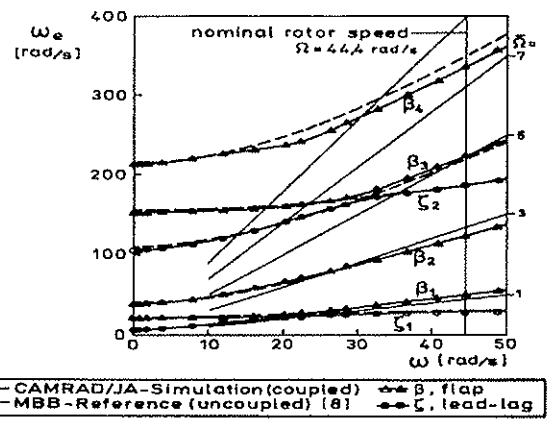

Fig. 8 : Southwell-Diagram of the Rotating and Fully Coupled Blade

In this way the eigen modes and eigen frequencies of the blade of the rotating system can be calculated. Analogous but seperate to this topic also the coupled torsion can be named. The specific behaviour of the rotor in fig. 8 can be pretty exactly expressed up to the forth natural flap frequency β_4 and because of that the solution of the *GALERKIN*-method [9] for 3 flap, 2 lag and 1 torsion modes can be considered as sufficiently precise [10].

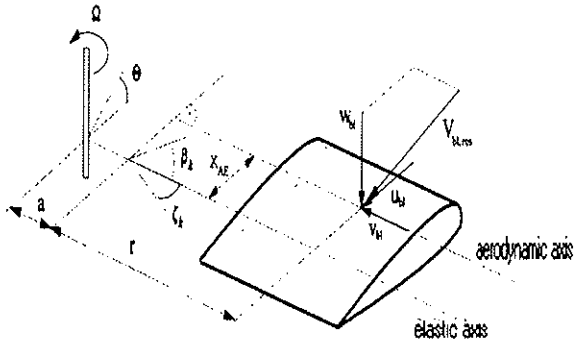

Fig. 9 : Geometry of the Rotor Blade

The introduction of geometrical marginal conditions such as precone and constructional sweep angle β_k, ζ_k and also the location of the elastic axis in dependence on the aerodynamic axis X_{AE} and others are introduced.

3.2. Aerodynamic Loads

The basis for the calculation of aerodynamic loads is the lifting line theory formed by a twodimensional airfoil characteristic of the profile NACA 23012 [11] in which the static lift, drag and moment for every blade element can be named in dependence on the Mach number and the angle of attack.
The influence of the yawing Λ and sweep angle ζ from inflow conditions and the blade bending is defined from an empirical correction by *JOHNSON* [5].

$$\cos \Lambda = \sqrt{\frac{v_t^2 + v_n^2}{v_t^2 + v_n^2 + v_r^2}} \qquad (6)$$

A factor of influence is produced by both angles

$$f_\varepsilon = \cos \zeta - \sin \zeta \tan \Lambda \qquad (7)$$

and the common balanced effect on the fixed aerodynamic coefficients.
Because the blades get also moved two-dimensional in the rotor disc during the horizontal rotation also

unsteady conditions have to be considered for the rotation. Also the dynamic stall at high blade angles gets satisfied by a semiempirical approach by *BEDDOES* [12].

$$C_{L,\mathrm{mod}}(\alpha) = \frac{C_L(\alpha f_\varepsilon \cos^2\Lambda)}{\cos^2\Lambda}$$

$$C_{D,\mathrm{mod}}(\alpha) = \frac{C_D(\alpha \cos\Lambda)}{\cos\Lambda} \qquad (8)$$

$$C_{M,\mathrm{mod}}(\alpha) = \frac{C_M(\alpha f_\varepsilon \cos^2\Lambda)}{\cos^2\Lambda}$$

The dynamic stall is characterized by the fact that the front line separation of the profile stream from the blade motion and loads delays depending on the rate of angle of attack.

$$\Delta C_L = \begin{cases} \Delta C_{Ld}\,(20\frac{\dot\alpha\, l}{V}) & \text{for } \frac{\dot\alpha\, l}{V} < 0{,}05 \\ \Delta C_{Ld} & \text{for } \frac{\dot\alpha\, l}{V} > 0{,}05 \end{cases} \qquad (9)$$

$$\Delta C_D = \begin{cases} 0 & \text{for } \frac{\dot\alpha\, l}{V} < 0{,}02 \\ \Delta C_{Dd}\,(33{,}3\frac{\dot\alpha\, l}{V} - 0{,}667) & \text{for } 0{,}02 < \frac{\dot\alpha\, l}{V} < 0{,}05 \\ \Delta C_{Dd} & \text{for } \frac{\dot\alpha\, l}{V} > 0{,}05 \end{cases} \qquad (10)$$

$$\Delta C_M = \begin{cases} \Delta C_{Md}\,(20\frac{\dot\alpha\, l}{V}) & \text{for } \frac{\dot\alpha\, l}{V} < 0{,}05 \\ \Delta C_{Md} & \text{for } \frac{\dot\alpha\, l}{V} > 0{,}05 \end{cases} \qquad (11)$$

This behaviour of hysteresis gets determined by dynamic correction factors for lift ΔC_L, drag ΔC_D , and pitching moment ΔC_M as soon as a given angle for beginning stall α_{st} is reached. The increase of the coefficients occurs just with a delayed angle α_d

$$\alpha_d = \alpha - \frac{\tau\, l}{|v_t|}\,\dot\alpha \qquad (12)$$

Start angle and time constant τ are modified through a synthesis by *JOHNSON* and *McCROSKEY* [13]. Unsteady effects because of chronological changes on the rotation plane are balanced for forces and moments at the thin and non stalled rotorblade, as follows [5].

$$\frac{L_{inst}}{l\, C_{L\alpha}} = sign(u_{bl})\left[\frac{l}{4}\, V_{bl,res}\,\dot\Theta\left(1+2\,\frac{x_{AE}}{l}\right) + \frac{l}{8}\left(\frac{dw_{bl}}{dt} + V_{bl}\,\frac{dw_{bl}}{dx}\right)\right] \qquad (13)$$

$$\frac{M_{inst}}{l\, C_{L\alpha}} = -sign(u_{bl})\left[\frac{l^2}{32}\, V_{bl,res}\,\dot\Theta\left(1+4\,\frac{x_{AE}}{l}\right)^2 + \frac{l^2}{32}\left(\frac{dw_{bl}}{dt} + V_{bl}\,\frac{dw_{bl}}{dx}\right)\left(1+4\,\frac{x_{AE}}{l}\right)\right] \qquad (14)$$

With this the pitch rate from control and blade motion is considered.

$$\dot\Theta = \frac{d\vartheta}{dt} + \beta + \mu\frac{d\vartheta}{dt}\cos\psi \qquad (15)$$

The drag changes in an analogous but not considerable manner.
Altogether the mentioned effects depend on the rotorflow and blade motion and have a big influence in the iterative process of the integration of thrust, moments and required power because they temporarily take care of more than 50% increase of the loads.

3.3. Rotor Wake Influence

The rotor downwash is mainly influenced by a small and medium speed through its own wake vorticity. It mainly depends on the dimension and the sort of the created circulation by *KUTTA-JOUKOWSKY* at the discreted blade element [14]

$$\Gamma_{res} = \frac{l}{2} v_{bl} C_L + \Gamma_{inst} \qquad (16)$$

with linear instationary part.

$$\frac{\Gamma_{inst}}{C_{L\alpha}\, l} = \frac{l}{4} \dot{\Theta} \left(1 + 2 \frac{x_{AE}}{l} \right) \qquad (17)$$

The development of these vortices is in this case created with a lattice of descreted straight line elements with viscous core radius for shed

$$\gamma_s = \frac{\delta \Gamma}{R\ \delta x} \qquad (18)$$

and trailed vorticity.

$$\gamma_t = - \frac{\delta \Gamma}{v_t\ R\ \delta \psi} \qquad (19)$$

The fixed points of these vortex lattice are forced into a stable position through the downwash conditions of their environment, which means through induced velocities of the rotor and environment by *BIOT-SAVART* in iterative steps [14]. The stable position corresponds to the downwash conditions of rotor wake.

$$\Delta \underline{w}_r = \frac{\Gamma}{4\ \pi} \oint \frac{\underline{r} \times d\underline{s}}{r^3} \qquad (20)$$

The simplification for the induction of finite straight vortex lines is as follows.

$$\Delta \underline{w}_r = \frac{\underline{r}_1 \times \underline{r}_2}{4\ \pi\ s_{seg}} \int_{s_1}^{s_2} \frac{\Gamma_m + s * \Gamma(s)}{(r_m^2 + s^2)^{\frac{3}{2}}}\, ds \qquad (21)$$

The final balance produces the downwash complex and therefore represents the steady incompressible flow conditions in the rotor disk.

Fig. 10 : Roll Up Process of the Helicopter Wake

Fig. 10 only presents the direction of movement of a single blade tip vortex. Because the influence of the wake vortices on the rotor declines quadratically with the distance the structure of the potential theoretical model can be simplified with the wake age. With this a limitation of compution time for the simulation can be achieved. The distribution of the angle of attack on the rotor disk results from fig. 11.

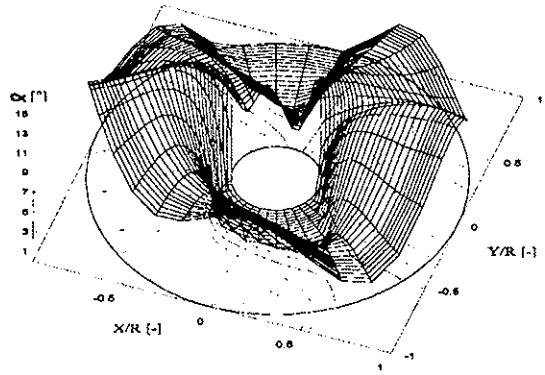

Fig. 11 : Angle of Attack Distribution with Performance Optimal HHC

The unsymmetrical conditions lead to unsteady phenomena during rotation and is the basis for the calculation of aerodynamic loads and blade vortex interactions of the simulation model.

3.4. Control Scheme of the Rotor Model

Beside the collective and cyclic rotor controls also multiple harmonics of the rotor frequencies are superpositioned.
The resultant pitch angle as a function of the rotation angle ψ and the blade coordinate x results from the blade twist Θ_{TW}, trim values such as Θ_0, Θ_C, Θ_S and the higher harmonic controls Θ_{nC}, Θ_{nS}.

$$\begin{aligned} \theta_{res} &= \theta_0 + \theta_{TW} + \theta_S \sin\Psi + \theta_C \cos\Psi \\ &\quad + \sum_{n=2} \theta_{nS} \sin n\Psi + \theta_{nC} \cos n\Psi \\ &= \theta_0 + \theta_{TW} + \theta_S \sin\Psi + \theta_C \cos\Psi \\ &\quad + \sum_{n=2} \hat{\theta}_n \cos(n\Psi - \Psi_n) \end{aligned} \qquad (22)$$

Because of the unsymmetrical inflow of the rotor the higher harmonic controls, especially 2Ω have got an influence on the trim conditions, which again has an effect on the reliability of the results. The aberrations

of the rolling moment of about a few hundred Newton-meters shows an almost complete compensation of the power gain through HHC-IBC at theoretic investigations and windtunnel tests in 1993. Nevertheless the simulation only uses a retrim algorithm which regards the flapping angle.
Furthermore the performance value of the rotor is a calculated scalar value and is not optimally controllable with a linear transfer function of periodical excitations. For this reason a free programmable, self-tuning freqency domain regulator was configurated for the numerical trimming of thrust load, roll- and pitch moments as well as for higher harmonic controls with optimum performance.
To obtain that goal is guaranteed through a cost function

$$J = (\underline{Z}_n - \underline{Z}_{targ})^T \underline{\underline{W}}_Z (\underline{Z}_n - \underline{Z}_{targ}) + \Delta\underline{\Theta}_n^T \underline{\underline{W}}_{\Delta\Theta} \Delta\underline{\Theta}_n \qquad (23)$$

with the convergence test criterion:

$$\sqrt{\Delta J} < \varepsilon \qquad (24)$$

The recursive solution effects the control function

$$\underline{Z}_n = \underline{Z}_{n-1} + \underline{\underline{\tilde{T}}} (\underline{\Theta}_n - \underline{\Theta}_{n-1}) \qquad (25)$$

with the gain matrix:

$$\underline{\underline{C}} = (\underline{\underline{\tilde{T}}}^T \underline{\underline{W}}_Z \underline{\underline{\tilde{T}}} + \underline{\underline{W}}_{\Delta\Theta})^{-1} \underline{\underline{\tilde{T}}}^T \underline{\underline{W}}_Z f \qquad (26)$$

The measurements are individually weighted against each other through the matrix $\underline{\underline{W}}_Z$ according to their estimated behaviour. The consideration of control weight matrix $\underline{\underline{W}}_\Theta$ as well as factor f can be regarded as damping components of this closed-loop-method. With these a stabilization of the response can be created.
Finally with a successful convergence in the regarded flight condition the linearized transfer behaviour supplies with the system matrix $\underline{\underline{T}}$ which is necessary for the design of a regulator including retrimming, results after convergency of the criterion.

4. Results and Discussion

The mentioned results and measurments from both windtunnel tests and simulations refer to a fullscale windtunnel model rotor of Bo105.
While the thrust loads reached up to 40000N and the speed up to 190kts in the expanded parameter studies (compare with fig. 3) the theoretical results were stated over the entire flight envelope with optimal controls dedicated to the described regulator.

4.1. Trim Error Due to HHC-IBC

On the basis of the unsymmetrical rotorflow a trim of the rotorsituation results at higherharmonic control (particularly 2Ω, large amplitudes). This situation has an unfavourable effect on the comparability of the performance data. The thrust and moment deviations were therefore compensated in the simulation as well as in measurements.

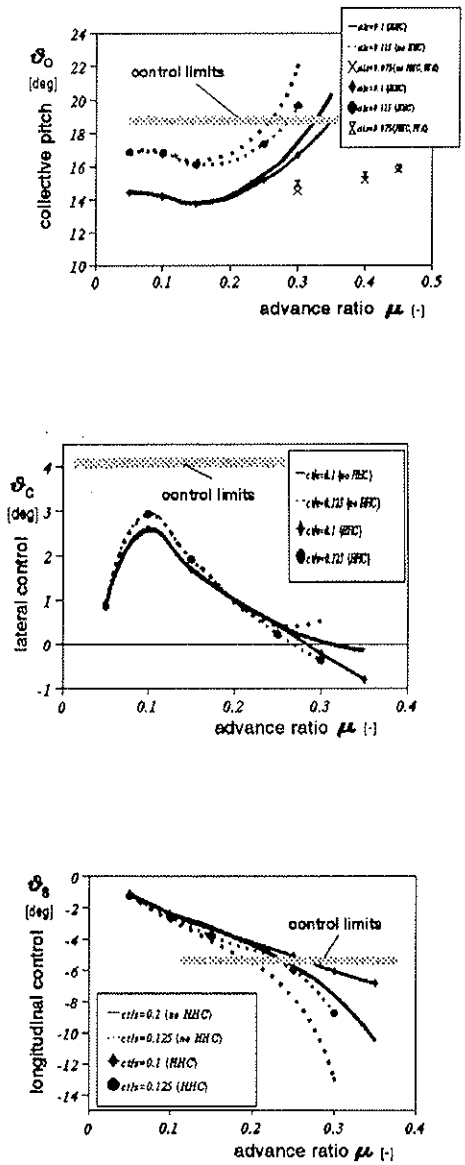

Fig. 12 : Retrim of the Rotor with Performance Optimal Control

Fig. 12 shows amplitude authority of the adaptations as a function of speed. Thrust, moments and rotor situation were kept corresponding to the equivalent flight situation in level flight. As can be see the collective controls combined with HHC were reduced because the rotor showed a bigger thrust efficiency. The behaviour is similar with the cyclic controls. In this way a higher control reserve was the conseqence. The windtunnel measurements showed an the other hand that a strong reversal of this effect can be expected at a non optimal control input.
Altogether retrim of target dependent optimal controls can be expected around 0.5°-1.5°. The tendency of the retrim obviously offers a higher stability reserve because values are decreased and the aerodynamic loads of advancing and retreating side got more distance to stall.

4.2. Vibration Reduction

To evaluate the effect of HHC-IBC on the vibration the Fast *FOURIER* Transformation (FFT) data of the rotor balance loads refered to the rotor hub were regarded.

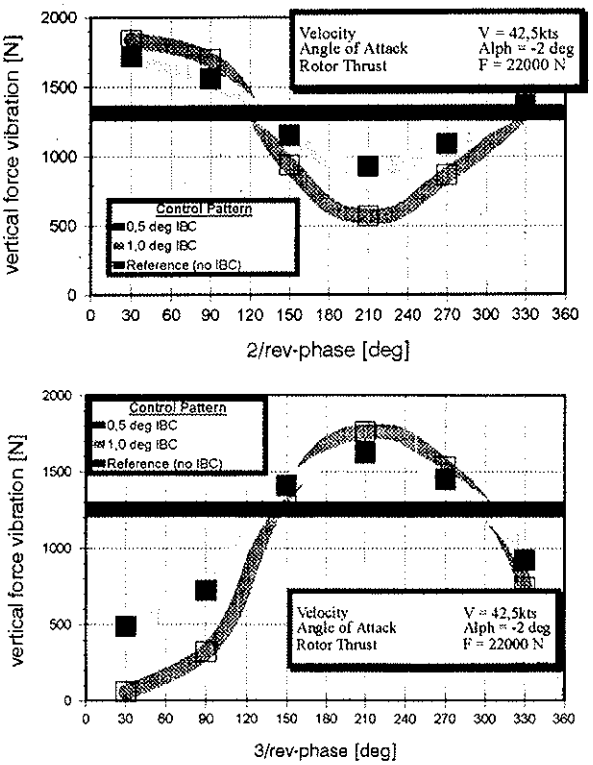

Fig. 13 : Vibration Reduction with HHC-IBC

For the four bladed rotor the 4Ω values of the shaft axis loads represent the effect of the helicopter vibration. The inputs of several flight conditions and IBC-authorities with frequencies from 2Ω to 6Ω are considered.
As we have also seen last year the 4Ω controls offered the biggest problem because the four parallel (or in phase) working actuators came very quickly to the duration limits of the conventional control system. For that reason only maximum amplitudes of 1° for the 4Ω excitation could be used.
In spite of this all other controls could be produced very exactly (ε<0.1°).

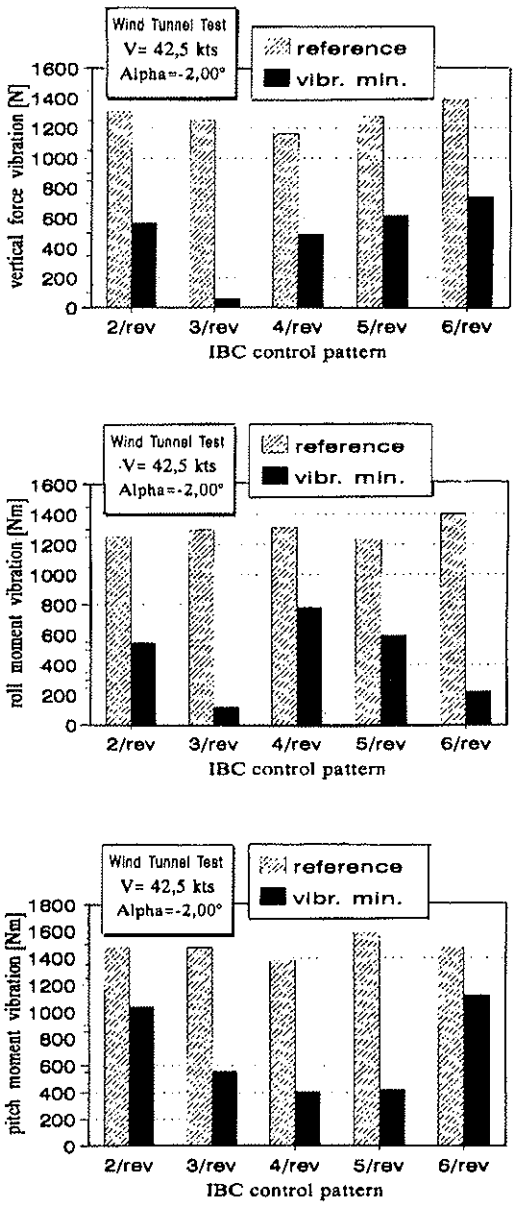

Fig. 14 : Vibration Dependent on Control Pattern

There has also been a number of other tests and investigations with HHC-controls of conventional limited systems. *SHAW* et al. [15] reported a 90% multicomponent suppression of vibrations with HHC-combinations. The optimal summarized amplitude

was named around 3° what came quite close to the RTA-results of 1994.
The phase shift of the measured and recalculated blade pitch developed between 0° and 14° and is likely a mistake from measurements and FFT-analysis, because the ZFL-monitoring for the controller showed much lower aberations.
In all cases the higher harmonic controls were able to reduce vibrations rapidly. With the higher advance ratio the optimal influence of the 2Ω control is seen more clearly. All responses seem to be proportional and linear with the input amplitude. In this way a linear transfer function can be expected.
In contrast to the measurements the simulation results are close in control response, but the baselines and effects at higher control amplitudes have certain aberations. This may be a consequense of the blade modification due to the measurement system. Another reason can be found in the idealized simulation which regards four identical and optimally tracked blades for all flight conditions.
The main advantage of IBC for vibration reduction is the fact that 5 load-component vibrations can be reduced by an equivalent number of controls. In this way we get a unique homogenous system of equation to get the optimal control constellation for complete vibration reduction.
As can be seen from fig. 14 all 1°-single-higher-harmonic-controls have got their own reducing effect between 30% and 90% on different components at different input phases.With a number of othogonal eigen vectors of the transfere matrix a complete optimal solution seems to be capable.

4.3 Offline Identification

The influence of the single harmonic control seem to prove a linear frequency domain behaviour without significant interharmonic couplings at small amplitudes.
After large test proceedings over the entire helicopter flight envelope it's time to create a general control algorithm for optimal vibration reduction. A complete offline system identifikation has to be performed and a continous transfer function has to be established.
First assumptions on a frequency domain were presented for the optimization of analytical models by *PAPAVASSILIOU, FRIEDMANN* and *VENTAKESSAN* [6] as a vibration reduction scheme for partly linear behaviour coupled with optimal control.
KLÖPPEL, TEVES and *RICHTER* [7] showed the idea of a continious identification of selected harmonic controls (3Ω-5Ω) with mixed control schemes. With the restriction of three control inputs the reduction of five load component harmonics would be difficult as the system of equations was limited. Because of the availability of uncorrected data the usage of this at lower velocities seemed to be not possible. After the second test phase this statement cannot be maintained.
As can be seen from the influence of the single harmonic controls every single harmonic excitation (2Ω-6Ω) got its own special effect on the vibration component of the hub loads. The following identification is done to built up the fundamental structure of a frequency domain closed loop controller for vibration reduction.
According to a linear behaviour of all 5 controls without interharmonic couplings of the effects a trigonometric function for the simultaneous reduction of all five vibration components of (X, Y, Z, M, N) can be developed. This assumption can be derivated from the behaviour of the single responses shown before and are written as

$$\underline{F}_{vib} = \underline{\underline{\hat{T}}}\,\underline{\Theta}_{IBC} + \underline{F}_{vib,basel} \qquad (27)$$

including all degrees of freedom in a static rotor condition of the windtunnel.
The influence of the harmonic controls seem to prove a linear transfer behaviour without any significant interharmonic couplings. After large test proceeding over the entire helicopter flight envelope it is time to build up a general control alogorithm.
The entire transfermatrix is build up by the superposition of the single harmonic 2x2-submatrices (for example $[T_x]_{n\Omega}$, means n^{th} input harmonic on X-load component).

$$\underline{\underline{\hat{T}}} = \begin{bmatrix} [T_X]_{2\Omega} & \cdots & [T_X]_{6\Omega} \\ \vdots & \ddots & \vdots \\ [T_N]_{2\Omega} & \cdots & [T_N]_{6\Omega} \end{bmatrix} \qquad (28)$$

The relation of one can be derived from the 4Ω-*FOURIER*-components of the hub loads, i.e.

$$\underline{X}_{vib} = [T_x]_{n\Omega} + \underline{X}_{vib,basel} \qquad (29)$$

with X_{vib} as the baseline drag vibration. Regarding the sin4Ω and cos4Ω components of the measured vibrations and the controls leading to this fig.15 shows a single transfer function. To get a complete behaviour at a determined flight condition all 25 submatrices have to be superpostioned.
It is a combination of translation of the baseline due to natural vibrations and unequal mechanical design, a phase shifting of the vibration output, the control

input, and at least an amplification effect dependent on the input direction.

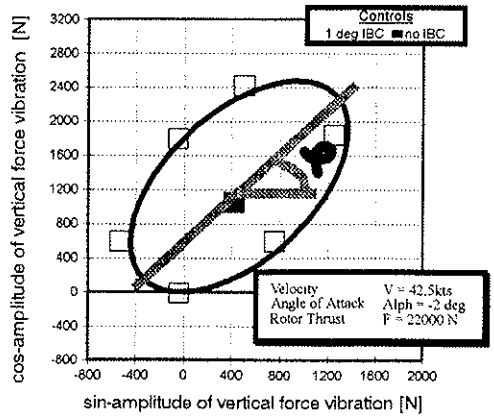

Fig. 15 : Vibration Response on Constant Amplitude HHC-IBC (2/rev, RTA-94)

To introduce all effects the following equation has to be solved for every component:

$$[F_{vib,\,targ}] = \begin{bmatrix} \cos\varphi & -\sin\varphi \\ \sin\varphi & \cos\varphi \end{bmatrix} \begin{bmatrix} a & 0 \\ 0 & b \end{bmatrix} [\vartheta_{n\Omega}] + [F_{vib,\,base}] \quad (30)$$

$$= \begin{bmatrix} a\cos\varphi & -b\sin\varphi \\ a\sin\varphi & b\cos\varphi \end{bmatrix} [\vartheta_{n\Omega}] + [F_{vib,\,base}] \quad (31)$$

Regarding one separat component we have got three unknown parameter in a system of two equations. Therefore we have to find out a third condition for the ellipsoidal relationship. To get this a parameter formula for the output ellipse is used to identify the position, orientation and dimension.

$$a\,F^2_{\cos 4\Omega} + 2\,c\,F_{\cos 4\Omega}F_{\sin 4\Omega} + b\,F^2_{\sin 4\Omega} + 2\,d\,F_{\cos 4\Omega} + 2\,e\,F_{\sin 4\Omega} = 1 \quad (32)$$

In this way the five parameters of a tilted ellipse *a* to *e* could be evaluated for all components of the hub loads. In this equation a and b are the amplification factors of the phase dependent inputs and

$$\varphi = \frac{1}{2}\arctan\left(\frac{2c}{a-b}\right) \quad (33)$$

the tilting (phase delay) angle of the rotor reaction. After the identification of the transfer function over the whole windtunnel envelope and in this way also the flight envelope it may be possible to get an entire behaviour on the harmonic excitation. The complete superpositioned matrix can be interpolated over the flight envelope and give an analytical pattern for the vibration control. The recursive advise makes

$$\underline{F}_{vib,\,targ} = \underline{\underline{T}}\,\underline{\Theta}_{IBC} + \underline{F}_{vib,\,meas} \quad (34)$$

Usually $\underline{F}_{targ}$ is suspected to be the required vibration free condition. According to this a control algorithm can be developed.

$$\underline{\Theta}_{IBC} = \underline{\underline{T}}^{-1}\left(\underline{F}_{vib,\,targ} - \underline{F}_{vib,\,meas}\right) \quad (35)$$

Out of this a technical closed-loop-regulation can be derived.

Because of the high influence of harmonic control it is recommended to integrate a retrim control. The transfer behaviour can also be estimated out of the measured data from the windtunnel. The estimated transfer matrix seems to be less dependent on the flight condition. Only the baseline vibration level has got serious influences from flight performance.

Nevertheless it is likely that a recoursive control pattern for the vibration reduction of the hub loads can be derivated for the entire flight envelope. The evaluation can be done by the mixed controls test point initiated by the NASA. The optimal controller that was testet in a quasi-closed-loop did not succeed for any task.

The main problem might have been the lack of previous controller tests and time problems for the software realization. For the next flight and windtunnel tests for the functionality of such a controller there may be better possibilites to prove it.

4.4. Performance Improvement with HHC-IBC

In former times theoretical investigations were made in the field of reduction of power requirement. The first analytical attempts showed very different results depending on kind and complexity of the theory and being almost not provable in general practice. In the presentation by *NGUYEN* and *CHOPRA* [16] a power gain reduction of 3-5% was claimed already for a minimum speed of 25 kts. *SHAW* [15] found this at a velocity of 40kts. *KRETZ* [17] determined more than 17% saving of power inside the normal flight envelope with an analytical method. A very optimistical assumption was set up by *WOOD* [18]. It claimed that the aerodynamical influences of the IBC-controls, independent of the kind and the performed flying speed, cause an improvement of the rotor efficiency

for a helicopter of the type OH-6A. However the measurements seem to be less reliable because they are not a periodic function of the rotary phase.
Against that *ROBINSON* and *FRIEDMANN* [19] came to the conclusion that in the entire considered flight envelope no reduction of rotor power can be achieved.
The here presented investigations and measurements which pass the permissible area of the actual Bo105 flight envelope showed effects which correspond to a mixture of the mentioned presentations. Shaft power reduction was realized in certain circumstances. But these only refered to the higher loaded rotor conditions without exception.

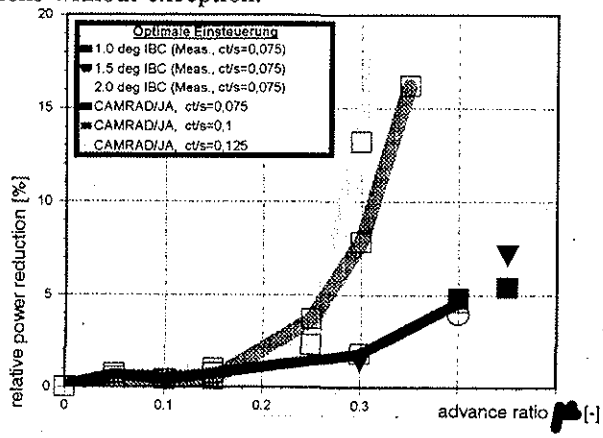

Fig. 16 : Shaft Power Reduction Due to HHC-IBC (Retrimmed)

As it is noticable in fig. 16 the power gain reduction at high speed and load are located at the best around 7%-10%. Proportional to the speed and the load the value reduces itself downward very quickly. For that reason considerable effects at medium load and speed are almost not to mention. Theoretical results and measurements agree very well.
Although the performance is strongly dependent on the shaft angle of attack deviations relative decreases are low.
At the same time vibrations and pitch link loads rise with optimal HHC-IBC control up to 20% but nevertheless they stay below the structural limit. At particularly high advance ratios reduction of loads of approximately 10% is noticable. Multiharmonical control inputs only showed an improvement in combination with a 2Ω-input.
On the basis of the increased expense at future investigations it should be fallen back on control methods which result from the overlapping part of the present results.
The single harmonic control input phase for optimal power gain and minimal vibration approach slowly with the advance ratio.
No considerable aerodynamic stall of the rotor was achieved in the measurements on the basis of NASA's load and control limitations, so that appropriate influence from the measurements is not avaluable.

4.5 Performance Balance

Finally a comparison of performance is carried out to find out in which way the power reduction can be compensated for HHC-IBC versus the need for the extra weight of the system (m_{IBC}=120kg) that is carried along and the hydraulic power and the power that is needed for controls.

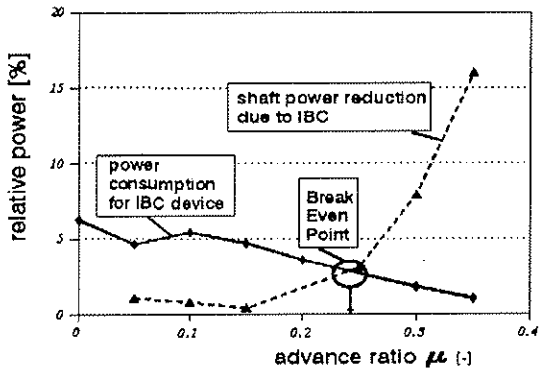

Fig. 17 : Performance Balance at CT/σ=0.1 Due to HHC-IBC

Corresponding to fig. 17 the point of intersection both results from calculated functions (Break Even Point) at a speed of approximately V_{kts}=100kts. Above this speed a corrected relative power saving of about 7% to 9% is reachable within the operational flight envelope.
This result is approximated on thrust loads corresponding to the maximum take off weight of MTOW=2650kg. But already at a medium load of 2100kg this effect would disappear within the normal velocity range (V_{kts} < 140 kts).

4.6. Noise Reduction

The wind tunnel configuration was also equiped to measure the noise level beneath the rotor model. For this item several fixed microphones and an array of others assembled on a movable traverse was installed (see fig. 4) to get the BVI-noise in dependence of the IBC-input.
There were different tests done from 2Ω to 6Ω as well as pulse, wavelet and doubled inputs. Not predicted but best reduction in all tests were done by the 2Ω-inputs.

As could be seen in several flight conditions with static and traverse running measurements the reduction of noise was realized over 8dB and mainly interfered by 2Ω-controls.
In fig. 18 a reduction at an extremely noisy recover condition (α=4°) could be found out. The mixed input of 2Ω and 5Ω offered the maximum reduction. This point was the optimum of the entire test and could not be improved with any of the closed loop tests performed by NASA. A year before *BROOKS* and *BOOTH* [20] got similar but less effective results with 4/rev-controls. Other inputs and mixed modes were considered as less effective. But nevertheless an IBC-system was discussed for better and most adaptive possibilities.
Although these results have been measured at a special rotor condition there were also other reductions in normal level flight conditions. The reductions were around 5dB of course but all showed a certain phase and amplitude behaviour as shown in Fig. 18.

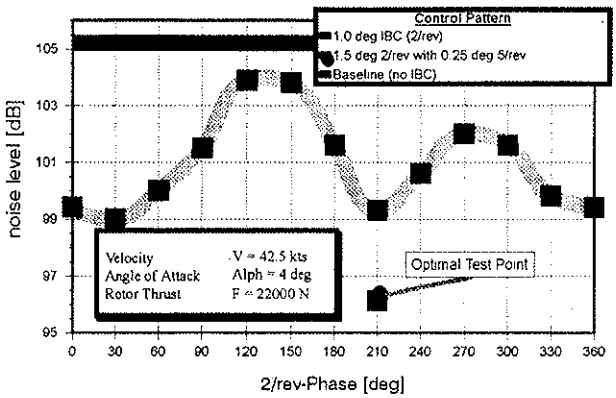

Fig. 18 : Noise Reduction with HHC-IBC

Concluding effects of all inputs in certain circumstances had an influence but especially 2Ω had the largest reduction of all.
The transfer function is obviously not linear and in this way it will take much more investigation to get an open-loop or even a closed-loop-control for single or multimode inputs.
Altogether the noise reduction between 4dB and 9dB seems to be a tremendous evidence for the further potential of the IBC-system.

5. Outlook and Conclusion

The presented investigations and tests were supposed to demonstrate the effect of HHC-IBC on vibration, performance and noise at helicopter rotors.
Contrary to the experiences with conventional limited HHC the variable IBC-systems made improvements independent from velocity and rotor condition possible at rather low authorities.
Vibrations can nearly completly be reduced by single controls for every load component and are likely to be minimized with linear analytical couplement of multiharmonic excitations of the blade pitch.
The simulation of those appearances with the required precision is achieved with methods that are rather extensive compared to conventional trim calculations. The reasons for that are fixed in the origin of the causal effects. It has to be assumed that they arise from a combination of unsteady aerodynamics, rotor inflow distribution and dynamic effects from high frequent controls and rotor blades. In that way a stall suppression is likely to supply with further improvements but could not be proved during the test, because safety limits of the windtunnel did not allow conditions like that.
The simulation which partly achieved good results in comparison to the measurements predicts larger improvements.
For the first time a reliable proof was given, that a limited reduction of the shaft power is possible through HHC-IBC maintaining the rotor trim condition. A real reduction of the power consumption at the Bo105 can only be considered at a speed of approximately V_{kts}>100 kts with high rotor loads. The retrim is achievable and leads to an increase of control and stability reserve. Altogether a reduction of shaft power and an additional load reduction at very high speed is provable.
Below that speed the system still shows significant effects on vibration and material load reduction as well as an effordable influence on BVI noise. In spite of the expected behaviour the biggest noise reduction (~9db) was achieved with a combined 2Ω-control.
This clearly holds the prospect of a task variable adaptive system. The required retrim can be ruled by coupled control.
Altogether with the proved technical reliance the active device is ready to finish developement for flying vehicles.
Future efforts will be mainly focused on the design of a closed-loop-regulator, the consolidation of the required technical reliability and combination of several different tasks with multiharmonic controls [18].
A long term aim now encouraged by successful experience but failed so far because of the required redundance is the entire taking over of complete tasks and elimination of the swashplate through the IBC-systems.

6. Acknowledgements

The tests dedicated in this study were performed for the German-American MOU-Task between NASA-Ames and ZF Luftfahrttechnik GmbH, Kassel, Germany.
Therefore we would like to thank Dr. William Warmbrodt (NASA) for his help to manage all logistic problems as well as Dr. Steven Jacklin (NASA) and Mr. Stephen Swanson (NASA) for their efforts on a successful performance and for aquisition of acoustic and dynamic test data.

7. References

[1] Wernicke, R.K.; Drees, J.M.
"Second Harmonic Control",
Bell Helicopter Company, Fort Worth, Texas, USA, 1964

[2] Richter, P.; Eisbrecher, H.D.
"Entwicklung und erste Tests von Aktuatoren für die Einzelblattsteuerung",
Sixteenth European Rotorcraft Forum, Glasgow, UK, Sept 1990

[3] Jacklin, S.A.; et al.
"Full-Scale Wind Tunnel Tests of A Helicopter Individual Blade Control System",
50th Annual National Forum of the American Helicopter Society, Washington DC, USA, 1994

[4] Peterson, R.L.; Maier, T.
"Corellation of Wind Tunnel And Flight Test Results of A Full-Scale Hingeless Rotor",
American Helicopter Society Aeromechanics Specialists Conference, San Francisco, CA, USA, 1994

[5] Johnson; W.
"CAMRAD/JA, A Comprehensive Analytical Model of Rotorcraft Aerodynamics and Dynamics",
Johnson Aeronautics, Palo Alto, CA, USA, 1988

[6] Pappavassiliou, I. et al.
"Coupled Rotor/Fuselage Vibration Multiple Frequency Blade Pitch Control",
Seventeenth European Rotorcraft Forum, Berlin, Germany, 1991

[7] Teves,D.; Klöppel,V.; Richter,P.
"Development of Active Control Technology in the Rotating System, Flight Testing And Theoretical Investigations",
18th European Rotorcraft Forum, Avignon, France, 1992

[8] Bayer, G.
"Zusammengestellte Daten zur Ermittlung von Ersatzsystemen, Biege- und Torsionsfrequenzen für den Bo105-Serienrotor mit Angabe der Ergebnisse",
Technische Niederschrift, TN-DE132-12/76,
MBB, Ottobrunn, 1976

[9] Houbolt, J.C.; Brooks, G.W.
"Differential Equations Of Motion For Flapwise Bending, Chordwise Bending, And Torsion of Twisted Nonuniform Rotor Blades",
NASA, Report 1346, USA, 1958

[10] Maier, T.H.
"An Examination of Helicopter Rotor Loads Calculations",
American Helicopter Society National Specialists, Meeting on Rotorcraft Dynamics, Arlington, Texas, USA, 1989

[11] Abbot, H.; Doenhoff, A.E. v.
"Theory of Wing Sections" NACA 23012",
Dover Publications,Inc, New York, 1959

[12] Beddoes, T.S.
"A Synthesis of Unsteady Aerodynamic Effects Including Stall Hysteresis",
Vertica, Vol. 1, No. 2, 1976

[13] McCroskey, W.J.
"Recent Developments in Dynamic Stall",
Symposium of Unsteady Aerodynamics,
Tucson, Arizona, USA, 1975

[14] Johnson, W.
"Helicopter Theory",
Princeton University Press, New Jersey, USA, 1988

[15] Shaw, J.; et al.
"Higher Harmonic Control: Wind Tunnel Demonstration of Fully Effective Vibratory Hub Force Suppression",
41th Annual National Forum of the American Helicopter Society, Forth Worth, Texas, USA, 1985

[16] Nguyen, K.; Chopra, I.
"Effects of Higher Harmonic Control on Rotor Performance And Control Loads"
AAIA 31st Structures, Structural Dymnamics and Material Conference, Long Beach, CA, USA, 1990

[17] Kretz, M.
"Active Expansion of Helicopter Flight Envelope",
15th European Rotorcraft Forum, Amsterdam, Holland, 1989

[18] Wood E.R.; Platzer, M.F.
"On the Computation of Helicopter Wake-Induced Unsteady Aerodaynamics Due to Higher Harmonics Control", Fifth Workshop on Dynamics Aeroelastic Stability, Modeling of Rotorcraft Systems, Rensellaer Polytechnic Institut, Troy, New York, USA, 1993

[19] Robinson, L.H.; Friedmann, P.P.
"A Study of Fundamental Issues in Higher Harmonic Control Using Aeroelastic Simulation",
American Helicopter Society National Specialists, Meeting on Rotorcraft Dynamics, Arlington, Texas, USA, 1989

[20] Brooks, T.F.; Booth, Jr. E.R.
"The Effects of Higher Harmonic Control on Blade Vortex Interaction Noise and Vibration",
Journal of the American Helicopter Society, Vol. 38, No. 3, July 1993